Aalborg Universitet

AALBORG UNIVERSITY

Current Control of Grid Converters Connected with Series AC Capacitor

Wang, Xiongfei; Blaabjerg, Frede; Loh, Poh Chiang; Pang, Ying

Published in:
Proceedings of the 30th Annual IEEE Applied Power Electronics Conference and Exposition, APEC 2015

DOI (link to publication from Publisher):
10.1109/APEC.2015.7104591

Publication date:
2015

Document Version
Early version, also known as pre-print

Link to publication from Aalborg University

Citation for published version (APA):
Wang, X., Blaabjerg, F., Loh, P. C., & Pang, Y. (2015). Current Control of Grid Converters Connected with Series AC Capacitor. In *Proceedings of the 30th Annual IEEE Applied Power Electronics Conference and Exposition, APEC 2015* (pp. 1800-1806). IEEE Press. https://doi.org/10.1109/APEC.2015.7104591

General rights
Copyright and moral rights for the publications made accessible in the public portal are retained by the authors and/or other copyright owners and it is a condition of accessing publications that users recognise and abide by the legal requirements associated with these rights.

- Users may download and print one copy of any publication from the public portal for the purpose of private study or research.
- You may not further distribute the material or use it for any profit-making activity or commercial gain
- You may freely distribute the URL identifying the publication in the public portal -

Take down policy
If you believe that this document breaches copyright please contact us at vbn@aub.aau.dk providing details, and we will remove access to the work immediately and investigate your claim.

Downloaded from vbn.aau.dk on: December 15, 2025

Current Control of Grid Converters Connected with Series AC Capacitor

Xiongfei Wang, Frede Blaabjerg, Poh Chiang Loh
Department of Energy Technology, Aalborg University
Aalborg, Denmark
xwa@et.aau.dk, fbl@et.aau.dk, pcl@et.aau.dk

Ying Pang
KK Wind Solutions a/s
Ikast, Denmark
yipan@kkwindsolutions.com

***Abstract*—The series ac capacitor has recently been used with the transformerless grid-connected converters in the distribution power grids. The capacitive characteristic of the resulting series *LC* filter restricts the use of conventional synchronous integral or stationary resonant current controllers. Thus this paper proposes a fourth-order resonant controller in the stationary frame, which guarantees a zero steady-state current tracking error for the grid converters with series *LC* filter. This method is then implemented in a three-phase experimental system for verification, where the current harmonics below the *LC* filter resonance frequency are effectively eliminated. Experimental results confirm the validity of the proposed current control scheme.**

***Keywords*—Series ac capacitor, current control, grid converter, transformerless active damper**

I. INTRODUCTION

Power electronic converters have increasingly been applied for grid integration of renewable power sources [1], energy efficiency improvement of electric power loads [2], and power quality enhancement in distribution power systems [3]. A low-frequency transformer with the step-down or step-up functions is usually needed for these grid-connected converters, which increases the system volume and weight. The transformerless ac/dc power converter with a series-connected ac capacitor has recently been reported in hybrid active filters and dampers [4]-[7], [11], [12], and in distributed generation systems [8]-[10]. Fig. 1 shows the general circuit diagrams of three-phase grid-connected voltage- and current-source converters with a series-connected ac capacitor C_g. This coupling capacitor can also be used together with the high-order *LC*/*LCL* filters in the voltage-source converters.

The series coupling capacitor is used to withstand most of the grid voltage, and thus reduces the voltage stresses of power components and the rated power of the converter [4]. Therefore it provides an alternative configuration for the transformerless grid-connected converters. However, this series capacitor also brings a number of challenges. First, the capability of power transfer, especially the output active power, is more sensitive to the size of capacitor than the normal grid converters with the coupling inductor [8]. Second, there is a coupling between the dc-link voltage regulation and reactive power control, which

This work was supported by European Research Council (ERC) under the European Union's Seventh Framework Program (FP/2007-2013)/ERC Grant Agreement [321149-Harmony].

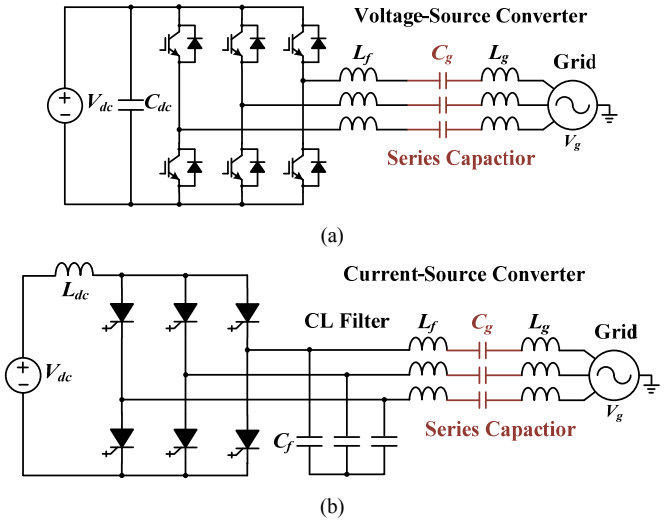

Fig. 1. Grid converters coupled with a series ac capacitor C_g. (a) Voltage-source converter [5]-[9]. (b) Current-source converter [4], [10].

affects the power controllability of the converter [11]. Third, the capacitive filter characteristic at those frequencies lower than the series *LC* resonance frequency challenges the use of usual synchronous integral and stationary resonant controllers. Those controllers are generally developed for the inductive filter "plant". It is shown that the direct use of conventional harmonic resonant controllers for the rejection of (5^{th} and 7^{th}) harmonic disturbances may destabilize the system.

To address these challenges, several research works have been reported. A quantitative analysis on the size of capacitor, dc-link voltage, and the transferred active power is given in [8]. Also, to mitigate the coupling between the dc-link voltage and reactive power control, the voltage in the middle of the series *LC* filter is controlled to operate the *L*-filtered converter as a voltage source. However, only a proportional current controller is employed to avoid the instability caused by the capacitive filter "plant". The resulting steady-state current tracking error has a little effect at the grid fundamental frequency, due to the use of Proportional-Integral (PI) controller for the outer dc-link and reactive power control. Yet the harmonic disturbance from the grid voltage, which may be lower than the filter resonance frequency, distorts the grid current injected by the converter. In [11], a hysteresis current control scheme is employed, where an adaptive dc-link voltage control method is developed for the

hybrid active filter to provide the dynamic reactive power compensation. The wide spectrum of current harmonics is however brought by the hysteresis modulation.

This paper therefore proposes a current control method for grid converters coupled with a series capacitor. A fourth-order resonant controller in the stationary frame is introduced for the zero steady-state current tracking error with the capacitive filter "plant". Thus, besides the control of the fundamental frequency current, the low-order harmonic currents, which may be caused by the grid harmonic voltages, the core saturation of the filter inductor, and the dead-time of the converter, can be eliminated effectively. It thus enables hybrid active filters to selectively reject or absorb harmonic currents at both the low- and high-frequencies. To validate the effectiveness of the approach, a laboratory system comprising a three-phase grid-connected voltage-source converter coupled with a series capacitor is built and tested. Experimental results demonstrate the performance of harmonic current compensation of the proposed controller.

II. Operation Principle

This section discusses the operation principle of a voltage-source converter coupled with a series capacitor to the power grid. The synthesis of the proposed current control scheme for a capacitive filter "plant" is illustrated.

A. System Description

Fig. 2 shows the overall control diagram for a three-phase grid-connected voltage-source converter with an *LC* filter and a coupling capacitor at the Point of Connection (PoC). The PoC voltage V_{poc} is measured for the grid synchronization by using a Phase-Locked Loop (PLL) in the synchronous reference frame [1]. The grid current that flows through the coupling capacitor is controlled in the stationary $\alpha\beta$-frame. Table I lists the main electrical parameters of the system.

Fig. 3 depicts the frequency response of the filter "plant" of the grid current control loop, which can be obtained based on the transfer function of the converter voltage to grid current.

$$Y_p(s) = \frac{i_g}{V_i}\bigg|_{V_{poc}=0} = \frac{C_g s}{L_f(C_f + C_g)s^2 + 1} \tag{1}$$

where it clearly shows that the "plant" has a phase shift of 90° below the resonance frequency of the filter, which indicates a capacitive characteristic at the fundamental frequency and the low-order (5th and 7th) harmonic frequencies.

To avoid the influence of the coupling between the dc-link voltage and reactive power compensation, the following two operating scenarios are considered in this work:

1) Controlled dc-link voltage with reactive current: The dc-link voltage is controlled by a PI controller, whose output is used as the reactive current command i_{gq}^*. The active current command i_{gp}^* is set to zero. In this case, the grid current cannot be controlled with zero steady-state error at the fundmental frequency, which will be discussed next. Hence, the proposed current controller is only applied to compensate the low-order harmonics.

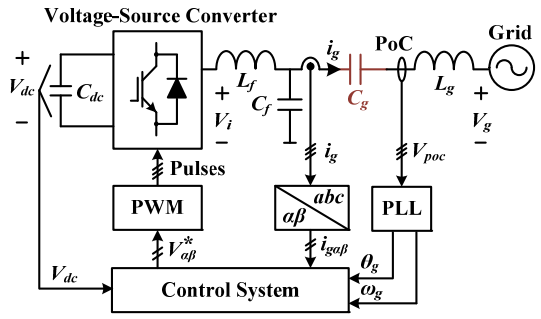

Fig. 2. Overall control of a grid converter with a series-connected ac capacitor.

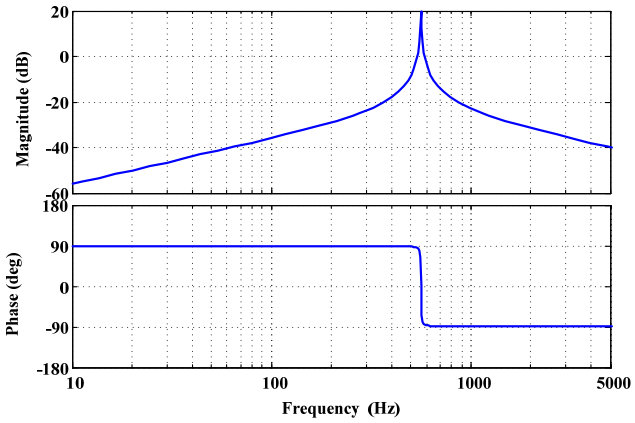

Fig. 3. Frequency response of the filter "plant" (see (1)) of the grid current control loop.

TABLE I
Main Electrical Parameters of the Grid Converter in Fig. 2

Symbol	Quantity	Value
V_g	Grid voltage	400 V
L_g	Grid inductance	1.8 mH
C_g	Series coupling capacitor	25 µF
V_{dc}	DC-link voltage	300 V
C_{dc}	DC-link capacitor	1600 µF
L_f	*LC*-filter inductor	2.7 mH
C_f	*LC*-filter capacitor	4.7 µF
f_{sw}	Switching frequency	10 kHz

2) Constant dc-link voltage: The dc-link voltage is in this case kept as constant by an external dc power source. Hence, the reactive current command i_{gq}^* is merely used for dynamic reactive power compensation. The fundamental frequency grid current can then be controlled with zero steady-state error.

Fig. 4 illustrates the block diagram of the Control System in Fig. 2, including the controllers for the dc-link voltage and reactive power, as well as the proposed fourth-order resonant current controller at the fundamental and low-order harmonics frequencies. These controllers are explained in the following.

B. Control of DC-Link Voltage and Reactive Power

Unlike the normal grid-connected converters coupled with the inductor, the dc-link voltage control here is realized by the

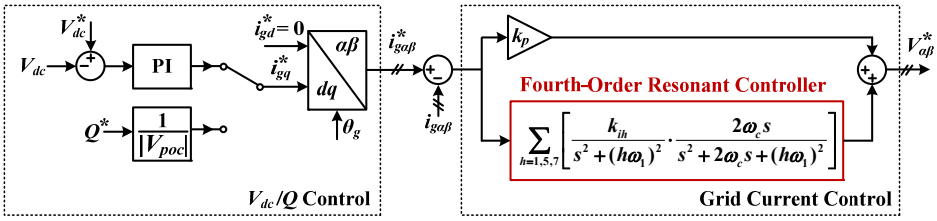

Fig. 4. Illustration of the Control System block of the grid-connected converter shown in Fig. 2.

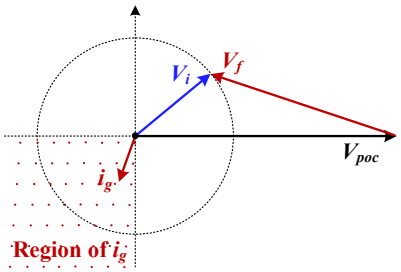

Fig. 5. A phasor diagram orientation of the converter at the grid fundamental frequency.

reactive current aligned to the orthogonal *q*-axis, rather than the active current along with the *d*-axis which the PoC voltage is aligned to. This is because the coupling capacitor is supposed to withstand most of the grid voltage, and the reactive current thus dominates the current injected into the grid [5]-[7].

However, it is important to note that the active current still exists to keep the dc-link voltage constant. Thus, even though the active current command is set to zero, there is still an active component in the actual grid current. Hence, the current control schemes with zero steady-state tracking error cannot be used at the fundamental frequency.

A phasor orientation diagram at the fundamental frequency is illustrated in Fig. 5, where V_f is the voltage across the passive filter, V_i is the converter output voltage. It is clear that V_f can only be in the second or third quadrant in order to be sure that $|V_i|$ is lower than the grid voltage at PoC $|V_{poc}|$. Further on, due to the 90° phase lead of grid current i_L over the voltage V_f, the allowed region of i_L is thus limited to the third quadrant [12].

On the other hand, with the dc-link voltage is kept constant, the reactive current command can be used to merely regulate the reactive power. By setting the active current command to zero, the reactive power is controlled by the proposed current controller with the zero steady-state error at the fundamental frequency. In this case, all the voltage phasors are in line with the V_{poc}, and the current is aligned to the orthogonal axis.

C. Proposed Current Control

The predominantly capacitive characteristic of the "control plant", which can be represented by an equivalent capacitance C_{eq} in the low-frequency range, is challenging the stability of using conventional synchronous integral or stationary resonant controller.

It is therefore necessary to re-shape the capacitive behavior by adding a second-order low-pass filter in series with the filter "plant", which is given in

$$Y_{op}(s) = C_{eq}s \Rightarrow Y_{rp}(s) = \frac{2h\omega_c}{s^2 + 2h\omega_c s + (h\omega_1)^2} C_{eq}s \tag{2}$$

where ω_1 is the grid fundamental frequency in rad/s. The term 'h' denotes the frequencies of interest (h = 1, 5, 7) in Fig. 3. $Y_{op}(s)$ and $Y_{rp}(s)$ are the transfer functions of the original and the reshaped "plants". The reshaped "plant" is thus changed as a band-pass filter with the common gain of C_{eq} at those frequencies. In other words, the re-shaped "plant" behaves like a resistor with the value of C_{eq}, hence allowing the use of the usual second-order resonant controllers without being burdened by the stability and dynamic concerns. The resulting controller becomes a fourth-order controller, which is given as

$$\begin{aligned} G_{2R}(s)\cdot Y_{rp}(s) &= G_{4R}(s)\cdot Y_{op}(s) \\ &= \sum_{h=1,5,7}\left\{\left[\frac{k_{ih}s}{s^2+(h\omega_1)^2}\right]\cdot\left[\frac{2h\omega_c s}{s^2+2h\omega_c s+(h\omega_1)^2}\cdot C_{eq}\right]\right\} \\ &= \sum_{h=1,5,7}\left\{\frac{k_{ih}s}{s^2+(h\omega_1)^2}\cdot\frac{2h\omega_c}{s^2+2h\omega_c s+(h\omega_1)^2}\right\}\cdot sC_{eq} \end{aligned} \tag{3}$$

where $G_{2R}(s)$ is the traditional second-order resonant controller, and $G_{4R}(s)$ is the proposed fourth-order resonant controller.

III. Frequency-Domain Analysis

To see the effectiveness of the proposed current controller, a simplified diagram of the grid current control loop is shown in Fig. 6. $G_d(s)$ represents the time delay involved into the digital control system. $Y_o(s)$ is the disturbance transfer function from the PoC voltage to the grid current. Thus, the open-loop gain of the current control loop $T(s)$ can be derived as:

$$G_c(s) = k_p + G_{4R}(s) \tag{4}$$

$$G_d(s) = e^{-1.5T_s s} \tag{5}$$

$$Y_o(s) = \frac{-i_g}{V_{pcc}}\bigg|_{Vm=0} = \frac{L_f C_f s^2 + 1}{L_f(C_f + C_g)s^2 + 1} \tag{6}$$

$$T(s) = G_c(s)G_d(s)Y_p(s) \tag{7}$$

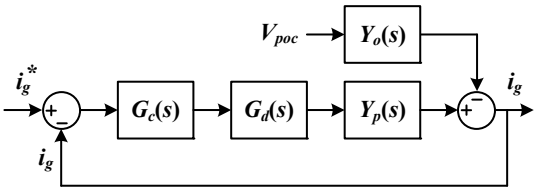

Fig. 6. Block diagram of grid current control loop.

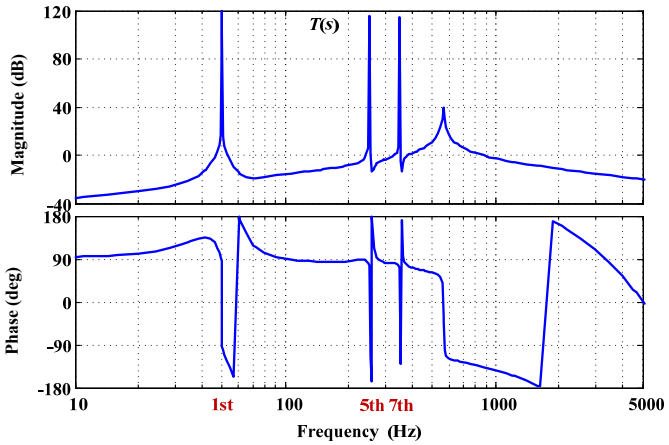

(a)

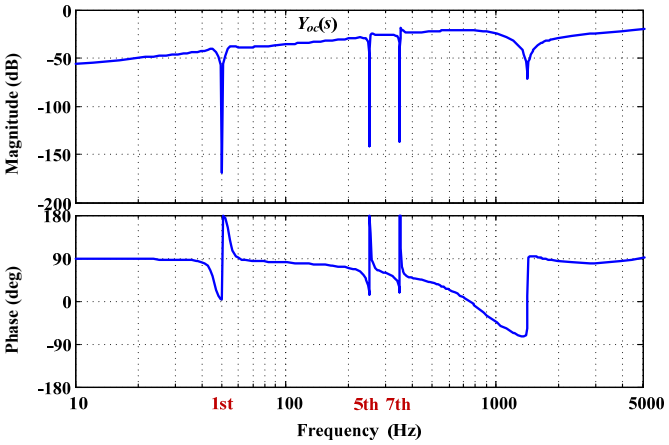

(b)

Fig. 7. Frequency responses of the grid current control loop. (a) Open-loop gain $T(s)$. (b) Closed-loop output admittance $Y_{oc}(s)$.

And the closed-loop output admittance $Y_{oc}(s)$ is given by

$$Y_{oc}(s) = \frac{Y_o(s)}{1 + T(s)} \tag{8}$$

Table II summarizes the main controller parameters used in the current control loop. The fourth-order resonant controller gains are dependent on the scale of the equivalent capacitance C_{eq}, hence they are chosen with very high values. Based on these parameters, the frequency responses of the open-loop gain $T(s)$ and the closed-loop output admittance $Y_{oc}(s)$ are drawn in Fig. 7. According to the Nyquist stability criterion, it can be seen

TABLE II
FOURTH-ORDER CURRENT CONTROLLER PARAMETERS

Symbol	Quantity	Value
T_s	System sampling period	100 μs
k_p	Proportional current controller	10
k_{i1}	Fourth-order resonant controller at the fundamental frequency	$1 \cdot 10^6$
k_{i5}	Fourth-order resonant controller at the 5th harmonic frequency	$1 \cdot 10^6$
k_{i7}	Fourth-order resonant controller at the 7th harmonic frequency	$4 \cdot 10^6$
ω_c	Cut-off frequency of the fourth-order resonant controller	31.4 rad/s

from Fig. 7 (a) that a stable grid current control is attained with the proposed controller. Moreover, from the closed-loop output admittance shown in Fig. 7 (b), a good rejection against the 5th and 7th harmonic voltage disturbances can also be observed.

IV. SIMULATIONS AND EXPERIMENTAL RESULTS

A. Simulations Results

To verify the effectiveness of the proposed control method, simulations based on the switching model of the grid converter shown in Fig. 2 are carried out using SIMULINK and PLECS Blockset. The parameters of the current controller and circuit constants given in Tables I and II are adopted. The parameters of the PI controller for the control of dc-link voltage are k_{p_d} = 0.8, k_{i_d} = 10. The grid voltage V_g is distorted with the -5th harmonic (0.01 p.u.) and the 7th harmonic (0.01 p.u.) voltages.

Fig. 8 shows the simulated grid current, PoC voltage, and dc-link voltage for the first operating scenario, i.e. controlling

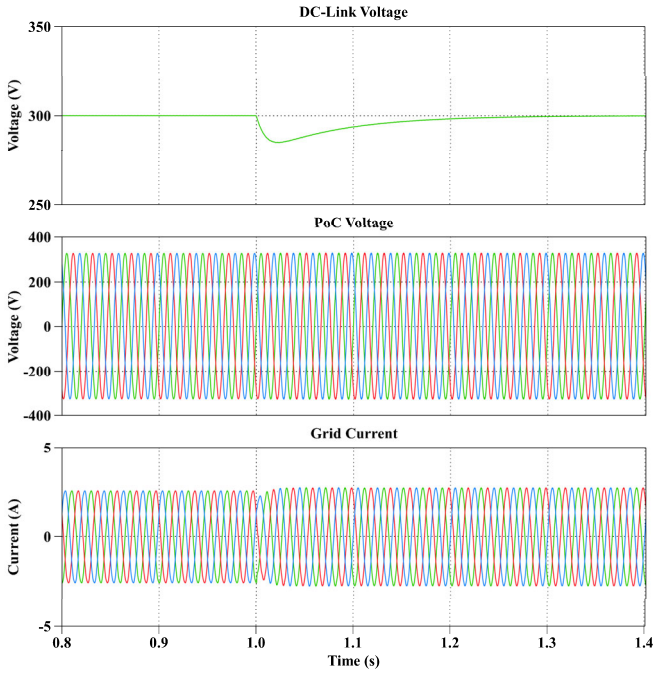

Fig. 8. Simulation results for the case of controlling dc-link voltage with a load step response at 1.0 s.

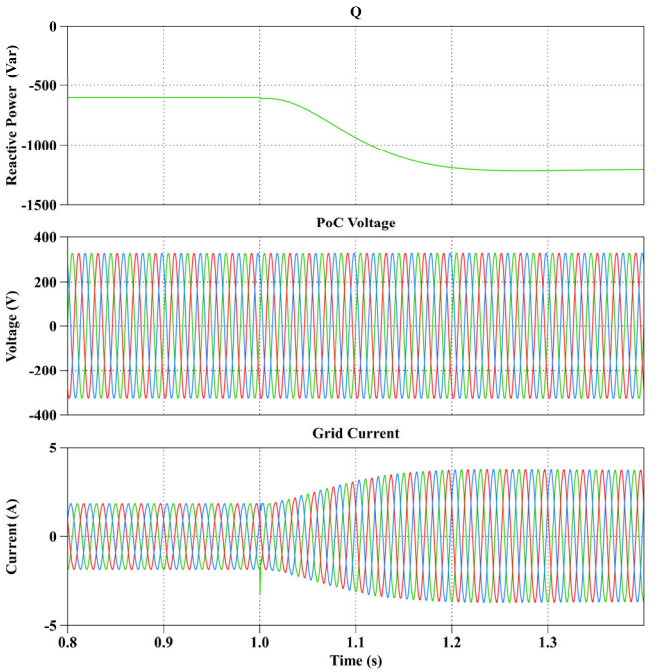

(a)

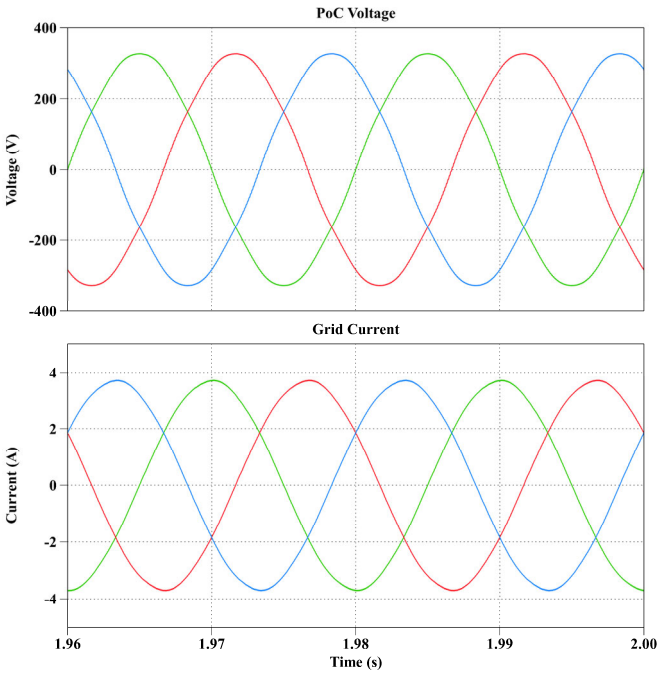

(b)

Fig. 9. Simulation results for the reactive power control with the constant dc-link voltage. (a) Step response of reactive power reference at 1.0 s. (b) Zoom-in view of PoC voltage and grid current at the steady-state.

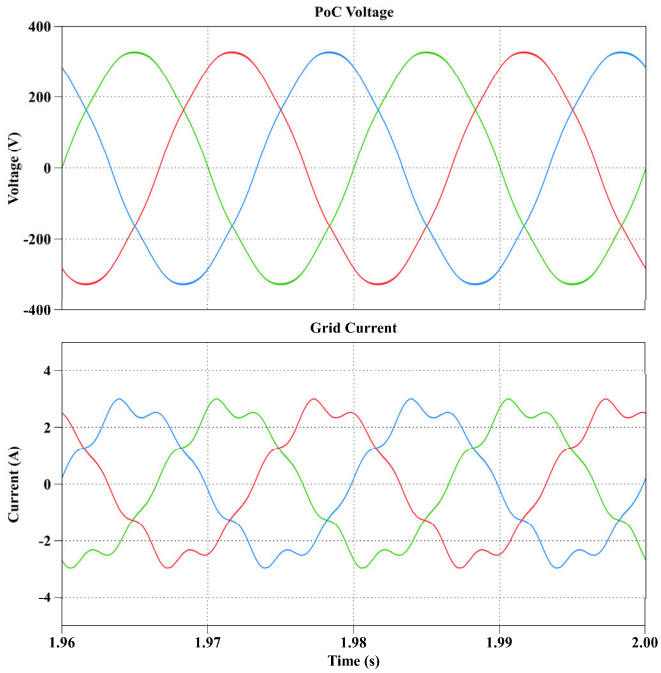

(a)

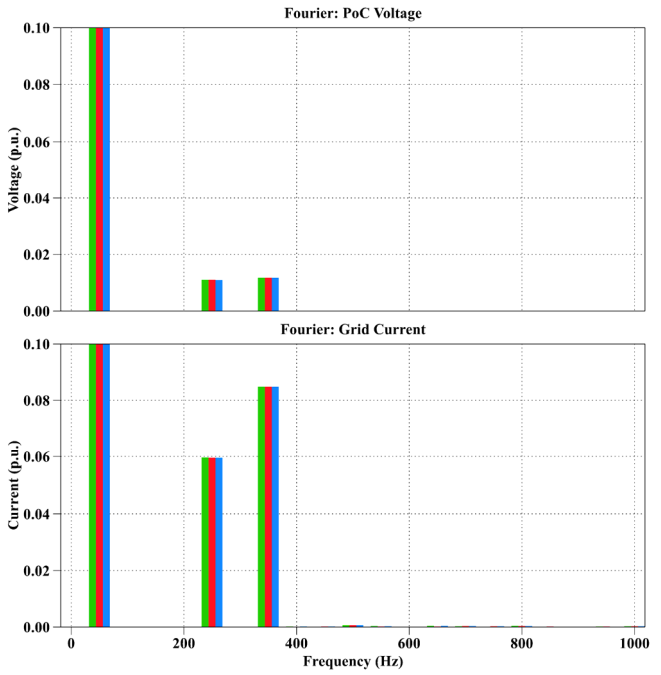

(b)

Fig. 10. Simulated grid current and PoC voltage and their harmonic spectra when only using the proportional current controller. (a) Simulated waveforms. (b) Harmonic spectra.

the dc-link voltage by the reactive current. In this case, a 150 Ω dc load is switched on at the time constant of 1.0 s. A reduced dc-link voltage with the closed-loop regulation is realized.

Fig. 9 shows the simulation results for the second operating scenario, i.e. the dc-link voltage is kept at 300 V by the dc voltage source. A step change of the reactive power reference from -600 Var to -1200 Var at 1.0 s is shown in Fig. 9 (a).

Fig. 9 (b) shows a zoom-in view of the simulated PoC voltage and grid current at the steady-state, where the 90° phase shift between them can be observed. It implies the zero steady-state tracking error at the fundamental frequency is attained by using the proposed fourth-order resonant current controller.

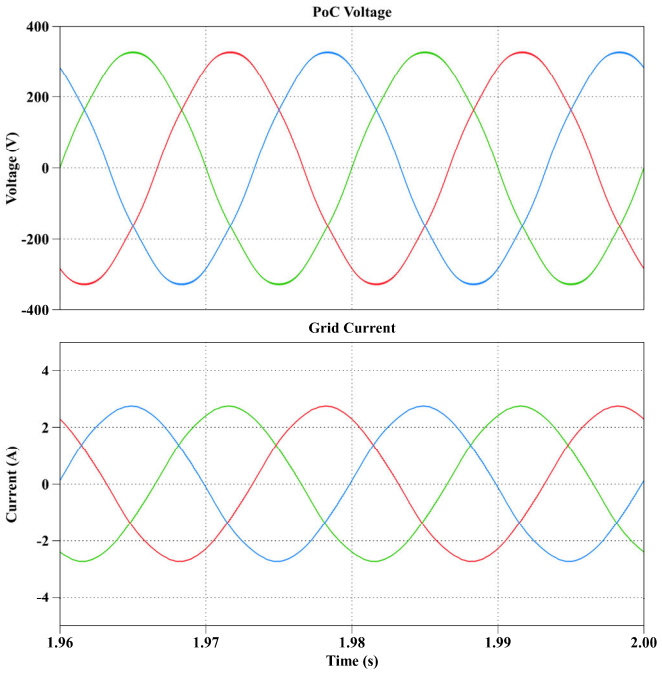

(a)

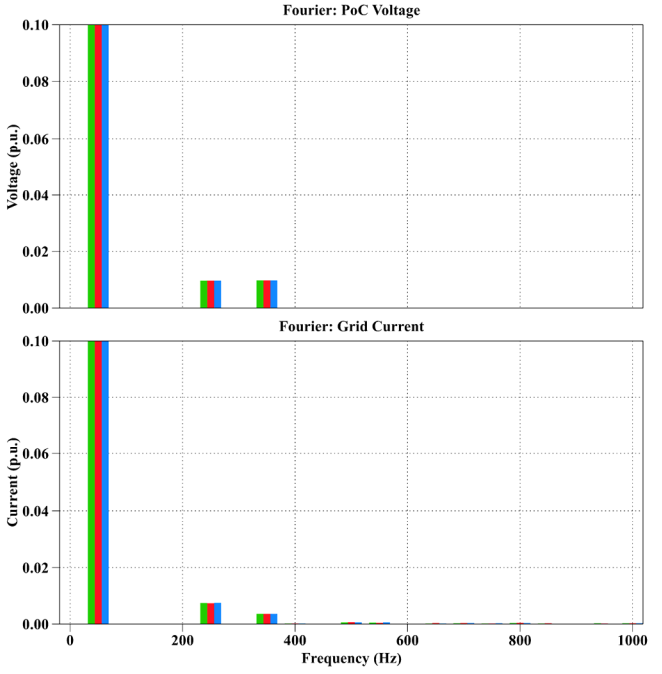

(b)

Fig. 11. Simulated grid current and PoC voltage and their harmonic spectra when using the proposed current control scheme. (a) Simulated waveforms. (b) Harmonic spectra.

Fig. 10 shows the simulated grid current and PoC voltage when only using the proportional current controller. From the harmonic spectra shown in Fig. 10 (b), it is seen that the grid current is severely distorted by the grid harmonic voltages. Hence, the current controller that guarantees zero steady-state error is important for compensating the current harmonics that are lower than the series LC filter resonance frequency.

Fig. 11 presents the simulated waveforms when using the fourth-order resonant controllers at the harmonic frequencies. It is clear that the grid current quality is significantly improved. Moreover, comparing the harmonic spectra shown in Fig. 11 (b) and Fig. 10 (b), an effective compensation of the harmonic currents by the proposed controller can be observed.

B. Experimental Results

To further verify the simulations results, a laboratory test system for the voltage-source converter shown in Fig. 2 is built with 2 μs dead-time in the power converter. Fig. 12 shows the hardware picture of the test setup, where the proposed control scheme is implemented into a dSPACE DS1006 system. The high-speed A/D sampling board DS2004 is used for sampling in synchronism with the digital Pulse Width Modulation (PWM) board DS5101. The parameters used in simulations are tested in experiments. The ac grid is emulated by the *California Instruments* MX-series AC power supply. However, instead of intentionally introducing the low-order harmonic voltages, the harmonic currents caused by the nonlinearity of dead-time are compensated in experiments.

Fig. 13 shows the measured dc-link voltage regulation and grid current. It can be seen that the dc-link voltage is reduced to the reference value after enabling the converter from the diode operation mode. The stable control of the dc-link voltage by the

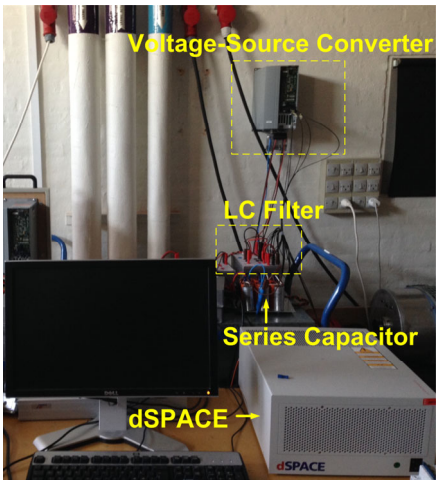

Fig. 12. Hardware picture of the laboratory test setup.

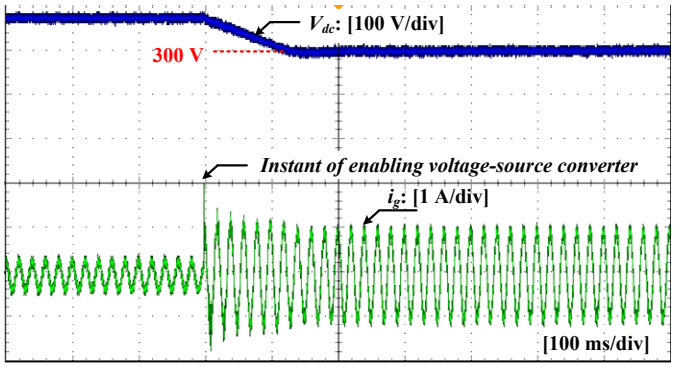

Fig. 13. Measured dc-link voltage and grid current in normal operation.

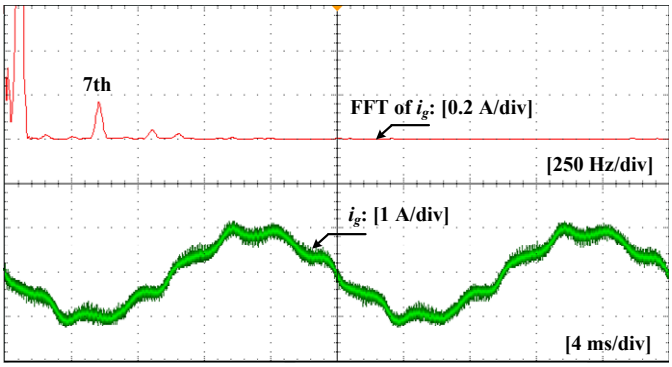

Fig. 14. Measured grid current and its harmonic spectra when only using the proportional current controller.

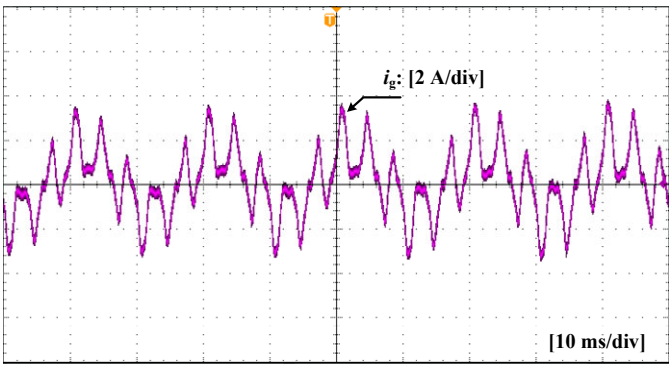

Fig. 15. Measured grid current and its harmonic spectra when using the usual second-order resonant controller.

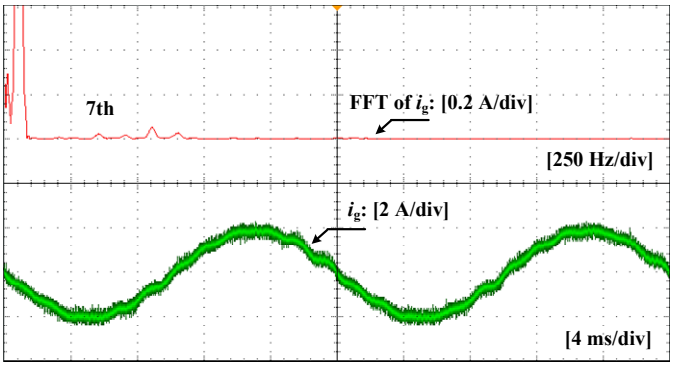

Fig. 16. Measured grid current and its harmonic spectra when using the proposed fourth-order resonant controller.

reactive current is thus validated.

Fig. 14 shows the measured grid current and its harmonic spectra when only using the proportional current controller. It is clear that the grid current is distorted by the 7th harmonic. Next Fig. 15 shows the measured grid current with the second-order resonant controllers, which are usually used for harmonic compensation. The harmonic distortion of the grid current becomes more severe, which indicates the instability of using the usual resonant current controllers for converters coupled by the ac capacitor. The measured grid current and its harmonic spectra after using the fourth-order resonant controller are then depicted in Fig. 16. An effective compensation of the 7th harmonic can be observed from the harmonic spectra, which confirms the validity of the proposed current control scheme.

V. Conclusions

This paper has presented a new current controller for grid converters coupled with series ac capacitor. Simulations and experimental results have demonstrated that the conventional resonant controllers cannot be applied for a capacitive "control plant". It is then necessary to re-shape the derivative filter by using the second-order transfer function, which together with the usual resonant controller, forms the proposed fourth-order resonant controller. It has been demonstrated that the proposed controller is important for the compensation of the low-order harmonics, which are below the resonance frequency of the output filter and the coupling capacitor. Experimental results obtained from a three-phase voltage-source converter verified the effectiveness of the proposed control scheme.

References

[1] F. Blaabjerg, R. Teodorescu, M. Liserre, and A. Timbus, "Overview of control and grid synchronization for distributed power generation systems," *IEEE Trans. Ind. Electron.*, vol. 53, no. 5, pp. 1398-1409, Oct. 2006.

[2] Y. Suh, J. K. Steinke, and P. K. Steimer, "Efficiency comparison of voltage-source and current-source drive systems for medium-voltage applications," *IEEE Trans. Ind. Electron.*, vol. 54, no. 5, pp. 2521–2531, Oct. 2007.

[3] H. Akagi, "Active harmonic filters," *Proc. IEEE*, vol. 93, no. 12, pp. 2128-2141, Dec. 2005.

[4] P. Parkatti, M. Salo, and H. Tuusa, "Modeling and measuring results of a shunt current source active power filter with series capacitor," in *Proc. EPE-PEMC* 2008, pp. 201-206.

[5] S. Srianthumrong and H. Akagi, "A Medium-Voltage Transformerless AC/DC power conversion system consisting of a diode rectifier and a shunt hybrid filter," *IEEE Trans. Ind. Appl.*, vol. 39, no. 3, pp. 874-882, May/Jun. 2003.

[6] S. Srianthumrong and H. Akagi, "Stability analysis of a series active filter integrated with a double-series diode rectifier," *IEEE Trans. Power Electron.*, vol. 17, no. 1, pp. 117-124, Jan. 2002.

[7] R. Inzunza and H. Akagi, "A 6.6-kV transformerless shunt hybrid active filter for installation on a power distribution system," *IEEE Trans. Power Electron.*, vol. 20, no. 4, pp. 893-900, Jul. 2005.

[8] T. L. Lee and Z. J. Chen, "A transformerless interface converter for a distributed generation system," in *Proc. IEEE EPE-PEMC* 2008, pp. 1704-1709.

[9] T. L. Lee, Z. J. Chen, and S. H. Hu, "Design of a power flow control method for hybrid active front-end converters," in *Proc. IEEE PEDS* 2009, pp. 133-138.

[10] C. Photong, C. Klumpner, and P. Wheeler, "A current source inverter with series connected ac capacitors for photovoltaic application with grid fault ride through capability," in *Proc. IEEE IECON* 2009, pp. 390-396.

[11] W. H. Choi, C. S. Lam, M. C. Wong, and Y. D. Han, "Analysis of dc-link votlage controls in three-phase four-wire hybrid active power filters," *IEEE Trans. Power Electron.*, vol. 28, no. 5, pp. 2180-2191, May 2013.

[12] X. Wang, Y. Pang, P. C. Loh, and F. Blaabjerg, "A series LC-filtered active damper for ac power electronics based power systems," in *Proc. IEEE APEC* 2015, in press.